Available online at www.sciencedirect.com
ScienceDirect
Journal of Photochemistry and Photobiology A: Chemistry 188 (2007) 252–259
Journal of Photochemistry and Photobiology A:Chemistry
www.elsevier.com/locate/jphotochem

Molecular structures and vibrations of *cis* and *trans m*-cresol in the electronically excited S_1 and cationic D_0 states

Jianhan Huang [a,c,*], Kelong Huang [a,*], Suqin Liu [a], Qiong Luo [a], Wenbih Tzeng [b]

[a] *College of Chemistry and Chemical Engineering, Central South University, Changsha 410083, China*
[b] *Institute of Atomic and Molecular Sciences, Academia Sinica, Taipei 10617, Taiwan*
[c] *The State Key Laboratory of Molecular Reaction Dynamics, Institute of Chemistry, Chinese Academy of Sciences, Beijing 100080, China*

Received 14 August 2006; received in revised form 6 November 2006; accepted 12 December 2006
Available online 16 December 2006

Abstract

The optimized molecular structures of *cis* and *trans m*-cresol in the ground S_0, electronically excited S_1, and cationic D_0 states are predicted by ab initio and density functional theory (DFT) calculations. Their vibrational spectra in the S_1 and D_0 states are recorded by two color resonant $(1+1')$ two photon ionization (2C-R2PI) and mass analyzed threshold ionization (MATI) methods. In consideration of the optimized geometries, the *trans* rotamer is more stable than the *cis* one in the S_0 state. Upon the $S_1 \leftarrow S_0$ excitation, the aromatic ring expansion is expected, and the interaction of the OH group with the ring is enhanced. On the $D_0 \leftarrow S_1$ transition, the bond length of the C1–O7 bond is further shortened, exhibiting a partial double bond character in the D_0 state. The band origins of *cis* and *trans m*-cresol are measured to be $35{,}982 \pm 2$ and $36{,}098 \pm 2\,cm^{-1}$ by the 2C-R2PI method, and their adiabatic ionization energies (IE) are determined to be $66{,}933 \pm 5$ and $67{,}084 \pm 5\,cm^{-1}$ by the MATI technique. Comparison of the IE of *o*-, *m*-, *p*-cresol, and phenol gives the order as: $p < o < m <$ phenol. Analysis of the spectroscopic features of *cis* and *trans m*-cresol in the S_1 and D_0 states shows that different orientations of the OH group with respect to the CH_3 group slightly influence the vibrational frequency of the in-plane ring deformation.

Keywords: Two color resonant two photon ionization (2C-R2PI); Mass analyzed threshold ionization (MATI); Band origin; Ionization energy (IE); Ab initio; Density functional theory (DFT)

1. Introduction

In the last two decades, there has been increasing activity in the field of the electronic spectroscopy of aromatic molecules with a methyl group [1,2]. By applying supersonic cooling technique, the vibronic spectra of these molecules are simplified and can give us the low frequency torsional transition related to the methyl internal rotation. Cresols (including *o*-, *m*-, and *p*-cresol) are good models to study the methyl internal rotation. They have OH and CH_3 groups which can act as active sites for many chemical reactions and hence have received many attentions in the photochemical and photophysical studies [3–5]. For *o*- and *m*-cresol, two conformers, *cis* and *trans*, arising from the different orientations of the OH group with respect to the CH_3 group at the *ortho* and *meta* position on the ring are expected, while only one structure is detected for *p*-cresol [3–10]. Cresols are also good models to investigate the substitution effect of the OH and CH_3 groups on the ring. The OH and CH_3 groups donate electron to the ring through σ bonds. In addition, the oxygen atom of the OH group shares its lone-pair electron with the ring, the CH_3 group interacts with the π-electron of the ring through hyperconjugation [11]. These interactions will result in some changes on the geometric structure and vibronic spectrum in the specific electronic states.

In the ground S_0 state, *m*-cresol has been investigated by IR [12] and dispersed laser induced fluorescence (LIF) [3,7] spectroscopy, and the normal vibrations have been assigned successfully. In the electronically excited S_1 state, excitation LIF [3,7], resonance enhanced multiphoton ionization (REMPI) [13,14], and hole-burning [15] spectroscopy have been applied to explore the spectroscopic properties of *cis* and *trans m*-cresol, their band origins are measured to be 35,980 and 36,099 cm^{-1},

* Corresponding authors at: College of Chemistry and Chemical Engineering, Central South University, Changsha 410083, China. Tel.: +86 731 8879850; fax: +86 731 8879850.
E-mail addresses: xiaomeijiangou@yahoo.com.cn (J. Huang), Klhuang@mail.csu.edu.cn (K. Huang).

1010-6030/$ – see front matter © 2007 Elsevier B.V. All rights reserved.
doi:10.1016/j.jphotochem.2006.12.016

and the methyl internal rotations such as 2e, $3a_1$, 4e, 5e, $6a_1$, and 7e are characterized in detail. In the cationic D_0 state, *cis* and *trans* *m*-cresol have been studied by the threshold $(1+1')$ resonant two photon ionization [13] and autoionization-detected infrared (ADIR) [16] spectroscopy, their ionization energies (IE) are measured to be 66,903 and 67,063 cm^{-1}, and the OH stretching vibrations together with the interaction of the OH group with the CH_3 group are determined.

Since the gap between the two band origins and two IE may differ by only a few tens to a few hundreds of wavenumbers for the two rotational conformers of *m*-cresol as well as some other molecules [17,18], a high resolution spectroscopic method with species selection capability is needed. Supersonic jet REMPI in conjunction with time-of-flight mass spectroscopy (TOF-MS) is an efficient method to probe the spectroscopic properties of molecules, complexes, and clusters [19–21]. The REMPI technique can not only lay out the vibrations in the excited state but also select a specific species from a mixture like the fingerprint for molecular identification. With the help of REMPI scheme, zero kinetic energy (ZEKE) [22] and mass analyzed threshold ionization (MATI) [23–25] spectroscopy can give the precise IE together with the vibrational even rotational spectrum of the selected rotamer in the D_0 state.

In this paper, we predict the optimized molecular geometries of *cis* and *trans* *m*-cresol in the S_0, S_1, and D_0 states by the restricted Hartree-Fock (RHF), configuration interaction singles (CIS), unrestricted Hartree-Fock (UHF), and density functional theory (DFT) methods. We also present two color resonant two photon ionization (2C-R2PI) and MATI spectra of the *cis* and *trans* rotamers of *m*-cresol, their band origins and IE are measured, assignments of the vibrations in the S_1 and D_0 states are attempted. Comparing these new data with those of *o*-cresol [10] and *p*-cresol [26], we can get an insight into the vicinal substitution effect of the OH and CH_3 groups.

2. Experimental and computational methods

2.1. Experimental method

The experiments were performed with a TOF-MS described elsewhere [26]. The *m*-cresol (Sigma, 99% purity) sample was heated to about 80 °C to acquire sufficient vapor pressure. The vapors were seeded into 2–3 bar of helium and expanded into the vacuum through a pulsed valve with a 0.15 mm diameter orifice. The pulsed valve was operated at 10 Hz with pulse duration of about 100 μs. The molecular beam was collimated by a skimmer located 15 mm downstream from the nozzle orifice.

The 2C-R2PI process was initiated by using two independent tunable UV lasers controlled by a delay/pulse generator (SRS DG535). The excitation dye laser (Lambda-Physik, Scanmate UV with BBO-I crystal; Coumarin 540A dye) was pumped by a pulsed frequency-tripled Nd: YAG laser (Quanta-Ray GCR-3). The UV laser output was directed perpendicularly into the molecular beam. The ionizing UV laser (Lambda-Physik, Scanmate UV with BBO-III crystal; DCM dye) was pumped by another frequency-doubled Nd: YAG laser (Quanta-Ray LAB-150). A Fizeau-type wavemeter (New Focus 7711) was used to calibrate the laser wavelength.

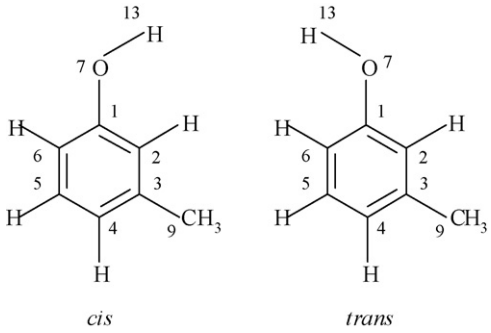

Fig. 1. The labeled scheme of *cis* and *trans* *m*-cresol.

In the MATI experiment, about 0.16 μs after the occurrence of the laser pulses, a pulsed electric field of −2.0 V/cm was switched on the first electric plate to separate the prompt ions from the high *n* Rydberg neutrals around the ionization region. About 11.6 ms later, a second pulsed electric field of about 120 V/cm on the second electric plate was applied to field-ionize the high n Rydberg neutrals. These high *n* Rydberg neutrals were ionized and the threshold ions were then accelerated to the detector.

2.2. Computational method

Ab initio and DFT calculations were performed by using the GAUSSIAN 03 program package [27]. The labeling of the carbon atoms of *cis* and *trans* *m*-cresol is 1–6 around the ring and the substituents are numbered as C1–OH and C3–CH_3, as seen in Fig. 1. Since the frequency calculation is on the basis of the harmonic oscillator model, the calculated frequencies are scaled by an appropriate value (0.90 for the S_1 state by the CIS/6-311G** method and 0.99 for the D_0 state by the B3PW91/6-311G** method) to correct approximately for the combined errors stemming from basis set incompleteness, neglect of electron correction, and vibrational anharmoncity. The IE was obtained from the difference in the zero point energy level of the D_0 and S_0 states.

3. Results and discussion

3.1. Stable rotamers of m-cresol in the S_0, S_1, and D_0 states: theoretical predictions

We have employed the RHF/6-311G**, B3LYP/6-311G**, and B3PW91/6-311G** methods to search the possible rotamers for *m*-cresol in the S_0 state. The initial molecular geometries contained the arrangements with the different orientations of the OH group from the CH_3 group. On the basis of these, the bond lengths, bond angles and dihedral angles were adjusted, and the optimized molecular structures were obtained by checking if there is no imaginary frequency. The results indicate that only two forms, the *cis* and *trans* rotamers, are stable, as shown in Fig. 1. The hydrogen atom of the OH group is in the benzene

ring plane for both of the *cis* and *trans* rotamers. In addition, the hydrogen atom of the OH group is at the C2 side for *cis m*-cresol, whereas the corresponding one is at the C6 side for *trans m*-cresol. Another important element of the molecular structure of *m*-cresol is the internal rotation of the CH_3 group which makes the two forms possible. In one form, one of the methyl C–H bonds at the C2 atom side is coplanar to the benzene ring. In another form, the C–H bond of the CH_3 group that is coplanar to the ring is at the C4 side. It may depend on the electronic and ionic states which form corresponds to the potential minimum.

In the S_0 state, the C–H bond of the CH_3 group coplanar to the ring is at the C4 side for *cis m*-cresol, while for *trans m*-cresol, the methyl C–H bond coplanar to the ring is at the C2 side. The calculated zero point energy levels of *cis m*-cresol are predicted to be −344.540847, −346.747995, and −346.610304 Hartree by the RHF/6-311G**, B3LYP/6-311G**, and B3PW91/6-311G** methods, respectively. Correspondingly, the ones of *trans m*-cresol are calculated to be −344.540979, −346.748071, and −346.610375 Hartree, respectively. It reveals that ab initio and DFT calculations give the same tendency that the total energy of *trans m*-cresol is lower than that of the *cis* rotamer by 29, 17, and 16 cm^{-1}, respectively, displaying the *trans* rotamer of *m*-cresol is more stable than the *cis* one in the S_0 state.

In the S_1 state, the methyl C–H bond coplanar to the ring is at the C4 side for *cis m*-cresol, and the optimized molecular geometry of *trans m*-cresol shows that the C–H bond of the CH_3 group coplanar to the ring is also at the C4 side. The $S_1 \leftarrow S_0$ transition energies of *cis m*-cresol are predicted to be 46,339, 39,040, and 39,228 cm^{-1} by the CIS/6-311G**, TD-B3LYP/6-311G**, and TD-B3PW91/6-311G** methods, respectively. The corresponding ones of the *trans* rotamer are measured to be 46,468, 39,350, and 39,319 cm^{-1}, respectively. It exhibits that the $S_1 \leftarrow S_0$ transition energies of the *cis* rotamer of *m*-cresol are redshifted from the *trans* one, which is helpful to assign the band origins of *cis* and *trans m*-cresol in the R2PI spectrum to be discussed later. In addition, the zero point energy levels in the S_1 state can be in turn calculated to be −344.329711, −346.570116, −346.431568 (for the *cis*), and −344.329255, −346.568779, −346.431224 (for the *trans*) Hartree, respectively. Thus, the total energy of *cis m*-cresol is lower than that of the *trans* rotamer in the S_1 state.

In the D_0 state, the optimized molecular structures of both of *cis* and *trans m*-cresol indicate that the methyl C–H bond coplanar to the ring is at the C2 side. The calculated zero point energy levels of *cis m*-cresol are determined to be −344.292049, −346.454167, and −346.315092 Hartree by the UHF/6-311G**, B3LYP/6-311G**, and B3PW91/6-311G** methods, respectively. The ones of the *trans* rotamers are prefigured to be −344.290892, −346.453324, and −346.314222 Hartree, respectively. Comparing the above data, it exhibits that the total energy of the *cis* rotamer is lower than that of the *trans* one by 254, 185, and 191 cm^{-1}, respectively, implying that *cis m*-cresol is more stable than the *trans* rotamer in the D_0 state. Comparing the zero point energy level of the *cis* rotamer based on the same calculation method in the D_0 and S_0 states, the IE of *cis m*-cresol can be calculated to be 54,605, 64,488, and 64,792 cm^{-1}, respectively. The ones of the *trans* rotamer can be calculated to be 54,888, 64,689, and 64,998, respectively, suggesting the IE of *cis m*-cresol is lower than the *trans* rotamer.

3.2. Molecular geometries of m-cresol in the S_0, S_1, and D_0 states

Table 1 lists the optimized structural parameters of *cis* and *trans m*-cresol by the RHF/6-311G**, CIS/6-311G**, and UHF/6-311G** calculations in the S_0, S_1, and D_0 states. In the S_0 state, the bond lengths of the C1–C2, C2–C3, and C3–C4 bonds of *cis m*-cresol are almost equal to the ones of the C6–C1,

Table 1
The bond lengths and bond angles of *cis* and *trans m*-cresol in the S_0, S_1, and D_0 states calculated by the RHF/6-311G**, CIS/6-311G**, and UHF/6-311G** methods, respectively

Bond lengths (Å)	*cis*			*trans*		
	S_0	S_1	D_0	S_0	S_1	D_0
C1–C2	1.382	1.414	1.416	1.390	1.412	1.423
C2–C3	1.393	1.413	1.360	1.382	1.412	1.360
C3–C4	1.384	1.418	1.446	1.395	1.415	1.440
C4–C5	1.390	1.409	1.404	1.378	1.413	1.412
C5–C6	1.377	1.410	1.373	1.388	1.408	1.366
C6–C1	1.389	1.413	1.443	1.382	1.417	1.442
C1–O7	1.350	1.328	1.281	1.351	1.328	1.279
C3–CH_3	1.510	1.498	1.499	1.510	1.499	1.501
O7–H13	0.940	0.942	0.949	0.940	0.942	0.949
Bond angles (°)						
∠C6C1C2	120.3	122.6	121.6	120.3	122.6	121.6
∠C1C2C3	120.7	118.6	119.4	120.6	118.9	119.7
∠C2C3C4	118.9	118.6	119.1	119.1	118.4	118.7
∠C3C4C5	120.0	122.6	121.6	120.1	122.5	121.8
∠C4C5C6	121.1	118.8	119.6	120.9	119.1	119.9
∠C5C6C1	119.0	118.7	118.7	119.1	118.4	118.3
∠O7C1C2	122.3	120.9	123.0	117.1	116.6	116.8
∠H13O7C1	110.6	110.8	114.8	110.6	110.9	115.0
∠C2C3C9	119.8	120.1	122.3	120.8	120.1	122.3

C5–C6, and C4–C5 bonds of the *trans* rotamer, implying the orientations of the OH group from the CH_3 group play an important role on the σ bond system of the benzene ring. The respective bond lengths of the C1–O7 and C3–CH_3 bonds are nearly the same for the two rotamers, suggesting the intensity of the interaction between the substituents and the ring is similar for the two rotamers. The O7C1C2 angle is larger than the O7C1C6 angle for *cis m*-cresol, while the relationship is reversed for the *trans* rotamer, implying the OCC angle of the "O–H bond side" is always larger than that of the opposite side regardless the position of the CH_3 group. This may be from the repulsion between the hydrogen atom of the OH group and the ring.

The $S_1 \leftarrow S_0$ transition is subjected to the $\pi^* \leftarrow \pi$ excitation of the benzene ring due to the population of anti-bonding orbital, and the ring expansion is expected [26,28]. When *m*-cresol is excited from the S_0 state to the S_1 state, the bond lengths of the ring CC bonds are all lengthened, while the ones of the C1–O7 and C3–CH_3 bonds are shortened by 0.022 and 0.012 Å for the *cis* rotamer, and by 0.023 and 0.011 Å for the *trans* rotamer. This indicates that the ring is really expanded on the $S_1 \leftarrow S_0$ excitation, whereas the interaction of the OH and CH_3 groups with the ring is enhanced in the S_1 state.

The $D_0 \leftarrow S_1$ transition corresponds to the removal of the lone-paired electron of the oxygen atom of the OH group for phenol and its derivatives [26,29]. The remaining non-bounded p-electron of the oxygen atom conjugates with the π electron of the ring. The bond lengths of the C1–O7 bond are shortened from 1.328 and 1.328 Å in the S_1 state to 1.281 and 1.279 Å in the D_0 state for *cis* and *trans m*-cresol, showing greater interaction between the OH group and the ring in the D_0 state. The typical bond lengths of the C–O and C=O bonds are reported to be 1.430 and 1.240 Å [11], it means that the C1–O7 bond of *cis* and *trans m*-cresol in the D_0 state exhibits a partial double character because of the p-electron delocalization of the OH group to the ring. Correspondingly, the bond lengths of the ring C2–C3 and C5–C6 bonds are shortened by 0.053 and 0.038 Å for the *cis* rotamer, and 0.052 and 0.042 Å for the *trans* one on the $D_0 \leftarrow S_1$ excitation, displaying a more intense conjugation, and the benzene ring forms a character of two short and four long bonds in the D_0 state. This configuration of *cis* and *trans m*-cresol in the D_0 state is somewhat similar to that of quinone.

3.3. 2C-R2PI spectrum of m-cresol displaying the vibrations in the S_1 state

Both of 1C-R2PI and 2C-R2PI techniques can record the vibronic features in the S_1 state. The latter approach was accomplished by fixing the ionizing laser at the laser energy of $D_0 \leftarrow S_1$ excitation while scanning the excitation laser in the range of near the $S_1 \leftarrow S_0$ transition. If the transition energy of the $D_0 \leftarrow S_1$ excitation is much less than that of the $S_1 \leftarrow S_0$ transition, there is a large number of excess energies for the 1C-R2PI scheme, leading to the bad signal-to-noise ratio. However, for the 2C-R2PI process, it has a less excess energy by a few thousand wavenumbers by introducing the second laser, it follows that some vibronic bands in the R2PI spectrum are more pronounced, as seen in Fig. 2. *m*-Cresol has 16 atoms, 42 normal vibrations containing 30 benzene-like, 3 OH group, and 9 CH_3 group vibronic modes. Concerning the active vibrations in the S_1 state, only those with large Franck–Condon overlaps can be observed in the R2PI spectrum. We assign the bands with frequencies at 35,982 and 36,098 cm^{-1} to the band origins of the *cis* (defined as 0^0 (*c*)) and *trans* (defined as 0^0 (*t*)) rotamers, which are in excellent agreement with the reported ones [7,13]. Certainly, the energy barrier between the two rotamers in the S_0 state is high enough that no transfer of population from the *cis* to the *trans* rotamer in the supersonic jet is expected [13], so the magnitude of the *cis* and the *trans* rotamer at the $S_1 \leftarrow S_0$ transition moment does not change in the course of the supersonic expansion of *m*-cresol, and the intensity ratio (I_c/I_t) of the 0^0 (*c*) and 0^0 (*t*) in the R2PI spectrum should reflect their relative abundances at the nozzle temperature. A simple relationship is expressed as $I_c/I_t = \exp(-\Delta E/kT)$, where ΔE is the energy difference between the *cis* and *trans* rotamers in the S_0 state, k is the Boltzmann constant, and T is the nozzle temperature. In Fig. 2, the intensity ratio (I_c/I_t) of the 0^0 (*c*) and 0^0 (*t*) in the R2PI spectrum is about 0.65 with our experimental temperature at 353 K, and then ΔE can be calculated to be about 470 cm^{-1}. This indicates that the total energy of the *trans* rotamer is lower than that of the *cis* one in the S_0 state. Although the calculated energy difference between the *cis* and *trans* rotamers is much larger than the theoretical one discussed in the previous section, the trend is the same. To correct the observed intensity ratio in the 2C-R2PI spectrum in Fig. 2 to the relative population of *cis* and *trans m*-cresol, one has to take into account some other factors. In the theoretical section, ab initio and DFT calculations have shown that the total energy of the *trans* rotamer is lower than that of the *cis* one by 29, 17, and 16 cm^{-1}, respectively. Upon the electronic transition, the *cis* rotamer may demonstrate a large change in geometry than the *trans* rotamer, which gives rise to different Frank–Condon factors for these two rotamers. Secondly, the electronic temperature may not be the same as the nozzle temperature as stated to be 353 K in our experiment. Because of these, the calculated energy difference of 470 cm^{-1} between *cis* and *trans m*-cresol in the S_0 state is much larger than the predicted ones by ab initio and DFT methods.

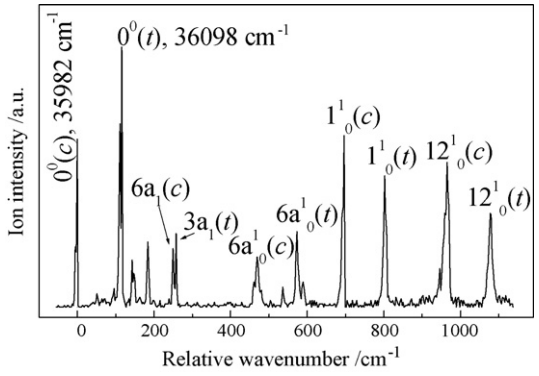

Fig. 2. 2C-R2PI spectrum of *m*-cresol. The band origins of the $S_1 \leftarrow S_0$ electronic transition for *cis* (*c*) and *trans* (*t*) *m*-cresol appear at 35,982 and 36,098 cm^{-1}, respectively.

Except for the methyl internal rotations such as 2e, $3a_1$, and $6a_1$ as reported in ref [13], we have also observed the vibra-

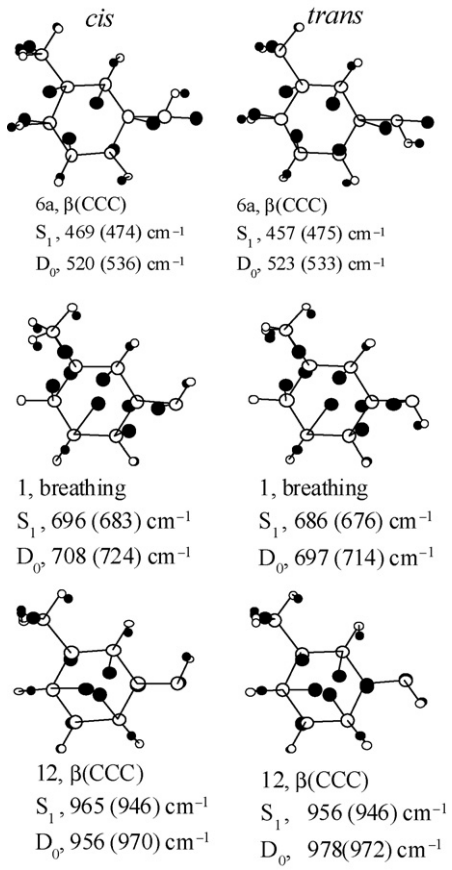

Fig. 3. The in-plane ring deformations of *cis* and *trans m*-cresol in the S_1 and D_0 states. The open circles designate the original locations of the atoms, whereas the solid dots mark the displacements. The measured and calculated (in the parentheses) frequencies are included for each mode.

tions related to the ring in the 2C-R2PI spectrum of *m*-cresol in Fig. 2. The intense bands corresponding to the $6a^1_0$, 1^1_0, and 12^1_0 transitions appear at 469, 696, and 965 cm^{-1} (for the *cis*), and at 457, 686, and 956 cm^{-1} (for the *trans*). This indicates that different orientations of the OH group from the CH_3 group slightly influence the frequency of the in-plane ring deformation in the S_1 state. As shown in Fig. 3, for these three modes, the motions of the respective atoms of *cis* and *trans m*-cresol are similar, displaying the relative orientations of the OH group with respect to the CH_3 group do not have an impact on the motions.

3.4. 2C-R2PI and MATI spectra of cis and trans m-cresol

Fig. 4 shows the 2C-R2PI spectra of *cis* and *tans m*-cresol obtained by ionizing via the $S_1 0^0$ state. It is noted that this 2C-R2PI process is different from that for recording the vibronic spectrum in the S_1 state stated previously. The present 2C-R2PI spectra were recorded by fixing the excitation laser wavelength at the respective $S_1 0^0$ levels for the *cis* and *trans* rotamers while scanning the ionizing laser from several hundred wavenumbers above to a few hundred wavenumbers below the ionization threshold, and the total ion current is collected. As seen in Fig. 4, analysis on the rising steps in the photoionization efficiency (PIE) curves of the 2C-R2PI spectra gives the respective IE of

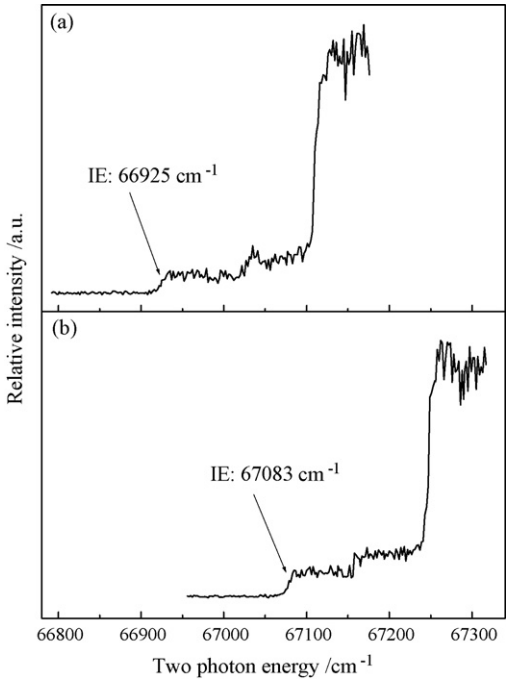

Fig. 4. 2C-R2PI spectra of (a) *cis* and (b) *trans m*-cresol via the $S_1 0^0$ state, the exciting laser energy was fixed by 35,982 and 36,098 cm^{-1} for the *cis* and *trans* rotamer while scanning the ionizing laser. The IE of the *cis* and *trans* isomers of *m*-cresol appear at 66,925 and 67,083 cm^{-1}, respectively.

these two rotamers to be 66,925 and 67,083 cm^{-1}, with an uncertainty of about 10 cm^{-1}, in good agreement with the reported ones [13].

In contrast to the 2C-R2PI method, the MATI technique gives a sharp peak at the ionization threshold and yields a more accurate IE. Since a small spoiling field is used to separate the prompt ions from the high n Rydberg neutrals before ionizing the high *n* Rydberg neutrals, the measured IE in the MATI method is a little lower than the true adiabatic IE of the molecule due to the Stark effect [30]. We have examined this phenomenon for *cis m*-cresol by recording the MATI signal via the $S_1 0^0$ state with the different spoiling fields at −0.8, −1.0, −1.2, −1.5, and −2.0 V/cm, respectively. The true IE can be obtained by plotting the measured IE as a function of $F^{1/2}$ (F is the magnitude of the spoiling field with the unit of V/cm) and extrapolating F to 0. As seen in Fig. 5, the slope of the fitted straight line is −3.98 and the intercept is 66,933 cm^{-1}, which indicates the lowing of the IE due to the Stark effect may be approximately to be 4.0 $F^{1/2}$ and the true adiabatic IE is 66,933 ± 5 cm^{-1} (8.2986 ± 0.0006 eV). With the same method, the IE of *trans m*-cresol can be determined to be 67,084 ± 5 cm^{-1} (8.3174 ± 0.0006 eV), in good agreement with those measured by the 2C-R2PI method.

Fig. 6(a and b) shows the MATI spectra of *cis* and *trans m*-cresol recorded by ionizing via the $S_1 0^0$ level. It can be seen that the general MATI spectral features of *cis* and *trans m*-cresol are similar. The pronounced MATI bands shifted from the ionization threshold (defined as 0^+) result from the active vibrations in the D_0 state. The active vibrations in the MATI spectra are related to the methyl internal rotations and the combination bands (the methyl internal rotation with the ring vibration) such as $6a_1 6a^1$,

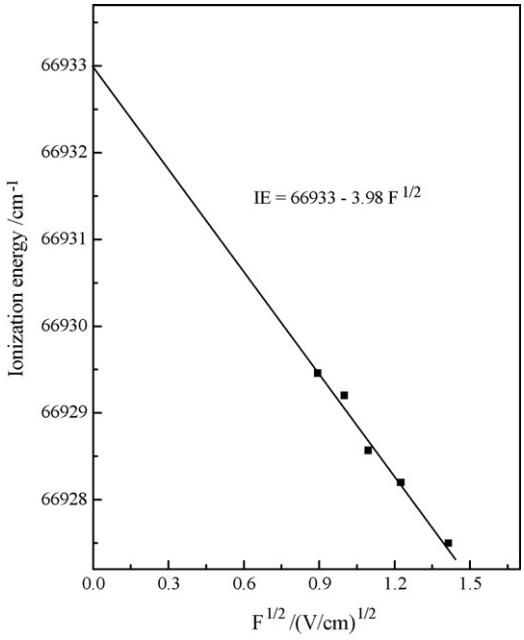

Fig. 5. The experimental observation of the lowing of the IE of *cis m*-cresol measured by MATI spectrum.

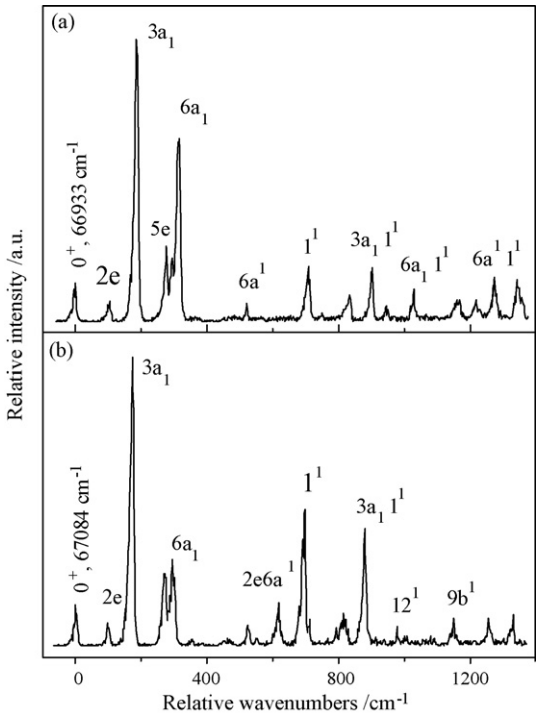

Fig. 6. MATI spectra of (a) *cis* and (b) *trans m*-cresol recorded by ionizing via the $S_1 0^0$ state.

$2e9b^1$, and $3a_1 9b^1$, respectively. All of the observed bands in the MATI spectra and their possible assignments are listed in Table 2, as well as the calculated vibrational frequencies with a scaling of 0.99 by the B3PW91/6-311G** method. As characterized by Mizuno et al. [13], the low-frequency bands result from the methyl internal rotation. Concernig the ring vibrations, the pronounced bands at 520, 708, and 946 cm^{-1} (for the *cis*), and 523, 697, and 978 cm^{-1} (for the *trans*) are assigned to the in-plane ring deformations 6a, 1, and 12, respectively. The substituent sensitive in plane C–OH bending vibration 9b appears at 1161 cm^{-1} (for the *cis*) and 1150 cm^{-1} (for the *trans*). These data indicate that the relative orientations of the OH group from the CH_3 group slightly affect the vibrational frequencies of these vibrations in the D_0 state.

Table 2
The observed vibrational bands of *cis* and *trans m*-cresol in the MATI spectra and possible assignments[a]

Cis			*Trans*			Assignments and approx. description[b]
Ref. [13]	This work	Cal	Ref. [13]	This work	Cal	
103	104	108	96	96	102	2e, τ(CH_3)
192	189		171	172		$3a_1$, τ(CH_3)
198			184			4e, τ(CH_3)
261	277		237			5e, τ(CH_3)
				271		$2e3a_1$
321	316		292	294		$6a_1$, τ(CH_3)
366			355			7e, τ(CH_3)
	520	536		523	533	$6a^1$, β(CCC)
				617		$2e6a^1$
	708	724		697	714	1^1, breathing
	834			817		$6a_1 6a^1$
	903			880		$3a_1 1^1$
	956	970		978	972	12^1, β(CCC)
	1029					$6a_1 1^1$
	1161	1142		1150	1146	$9b^1$, β(C–OH)
	1219	1188			1182	$18b^1$, β(CH)
	1275			1256		$2e9b^1$
	1343			1331		$3a_1 9b^1$

[a] The experimental values are shifted from the IE of the *cis* (66,933 cm^{-1}) and *trans* (67,084 cm^{-1}) rotamers of *m*-cresol. The calculated vibrational frequencies are obtained from the B3PW91/6-311G** calculation, scaled by 0.99.

[b] τ—methyl torsion, ν—stretching and β—in-plane bending.

Table 3
The experimental transition energies (in cm^{-1}) of phenol (aniline) and its derivatives[a]

Molecule	$S_1 \leftarrow S_0$	ΔE_1	$D_0 \leftarrow S_1$	ΔE_2	IE	ΔIE
Phenol [31]	36,349	0	32,276	0	68,625	0
Cis o-cresol [16]	36,421	72	30,434	−1842	66,855	−1770
Trans o-cresol [16]	36,205	−144	30,580	−1696	66,785	−1840
Cis m-cresol (this work)	35,982	−367	30,951	−1325	66,933	−1692
Trans m-cresol (this work)	36,098	−251	30,986	−1290	67,084	−1541
p-Cresol [26]	35,331	−1018	30,587	−1689	65,918	−2707
Aniline [32]	34,029	0	28,242	0	62,771	0
o-Methylaniline [33]	34,318	289	26,684	−1588	61,002	−1269
m-Methylaniline [33]	33,832	−197	27,227	−1015	61,059	−1212
p-Methylaniline [33]	33,084	−945	27,076	−1166	60,160	−2111

[a] ΔE_1, ΔE_2, and ΔIE are shifts of $S_1 \leftarrow S_0$, $D_0 \leftarrow S_1$, and IE with respect to those of phenol (aniline).

3.5. Vicinal effect on the electronic transition and ionization of o, m, and p-cresol as well as o, m, and p-methylaniline

For all the structural isomers, *o*, *m*, and *p*-cresol, the O–H is coplanar to the benzene ring plane, as in the case of phenol [31]. Although the CH_3 group at different position on the ring does not affect the planarity of the OH group, it can influence the interaction of the CH_3 group with the ring and will result in different π-electron density of the ring. The interaction between the CH_3 group and the ring may result from the inductive effect through σ bond and the resonant effect through π orbital. The inductive effect is related to the ability of donating or accepting electron of the substituents, while the resonant effect reflects the extent of π orbital overlap of the substituents with the ring. The collective effects lead to some changes of the surrounding electron density on the ring, following great changes of the zero point energy level of the electronic states.

As shown in Table 3 [16,26,31–33], the band origin of *cis o*-cresol is blueshifted by 72 cm^{-1} with respect to that of phenol, whereas the ones of the other structural isomers of cresol are all redshifted. Similarly, the band origin of *o*-methylaniline is blueshifted by 289 cm^{-1} from that of aniline, whereas the ones of the other structural isomers of methylaniline are all redshifted. As mentioned in the previous section, the $S_1 \leftarrow S_0$ excitation is mainly subject to the $\pi^* \leftarrow \pi$ transition of the ring, giving rise to some changes in the π-electron density around the ring. The difference of the transition energy reflects the degree of the change in the π-electron density around the ring on the $S_1 \leftarrow S_0$ transition. The red shift of the *m*- and *p*-methyl substitution for phenol (aniline) suggests that the interaction of the CH_3 group with the ring becomes stronger in the S_1 state than that in the S_0 state, consistent with the theoretical section. On the other hand, the $D_0 \leftarrow S_1$ transition corresponds to the removal of the lone-pair electron of the oxygen atom for phenol derivatives or that of the nitrogen atom for aniline derivatives. This step gives rise to a red shift in the transition energy for all the methyl substituted phenol and aniline as seen in Table 3. A possible interpretation is that the electron-donating CH_3 group causes an increase in the electron density nearby the ring and hence the OH (NH_2) group, resulting in less transition energy.

As the ionization process includes the $S_1 \leftarrow S_0$ and $D_0 \leftarrow S_1$ transition, the resulting IE of these methyl substituted phenol and aniline follows the order as: $p < o < m <$ phenol (aniline). It is reported that the IE of *o*-, *m*-, *p*-fluorophenol are 70,006, 70,188 (*cis*, *meta*), 70,449 (*trans*, *meta*), and 68,577 cm^{-1} [34–36], and the ones of *o*-, *m*-, *p*-fluoroaniline are reported to be 63,644, 64,159, and 62,543 cm^{-1} [37], respectively. In addition, the IE of *o*-methoxyphenol is determined to be 63,995 cm^{-1} [36], and those of the three rotamers of *m*-methoxyphenol are reported to be 64,741, 65,228, and 65,648 cm^{-1} [38], respectively. The IE of *cis*- and *trans*-*p*-methoxyphenol are measured to be 62,313 and 62,210 cm^{-1} [39]. This shows that the IE of *o*-, *m*-, *p*-fluorophenol, fluoroaniline, and methoxyphenol follows the same order as: $p < o < m$ as that of *o*-, *m*-, *p*-methylphenol and methylaniline.

3.6. Molecular vibration of cis and trans m-cresol

According to the numbering system of benzene-like vibrations in Varsanyi system [12], *m*-cresol is defined as 1, 3-dilight substituted benzene. Previous studies have shown that the in-plane ring deformations 6a, 1, and 12 are active for many of

Table 4
The observed vibrational frequencies (in cm^{-1}) of the in-plane ring deformation of phenol, *m*-cresol, and *m*-aminophenol in the S_1 and D_0 states

Molecules	Vibrational modes in S_1			Vibrational modes in D_0		
	6a	1	12	6a	1	12
Phenol [31]	475	935	796	521	973	805
Cis m-cresol (this work)	469	696	965	520	708	956
Trans m-cresol (this work)	457	686	956	523	697	978
Cis m-aminophenol [40]	466	721	960	535	748	979
Trans m-aminophenol [40]	475	714	963	527	748	973

these di-substituted benzenes in the S_1 and D_0 states. Table 4 lists the observed vibrational frequencies of modes 6a, 1, and 12 for phenol [31], *cis* and *trans* *m*-cresol, and *cis* and *trans* *m*-aminophenol [40] in the S_1 and D_0 states. Obviously, the vibrational frequencies in the S_1 state are less than those in the D_0 state for these three molecules. This suggests that the molecular geometry is less rigid in the S_1 state than that in the D_0 state, supported by the theoretical section state previously. In addition, the vibrational frequencies of the same mode between *m*-cresol and *m*-aminophenol are different in the S_1 and D_0 states, showing the nature of the substituent at the same position slightly influences the in-plane ring deformation. Comparing the vibrational frequencies of the same mode among phenol, *m*-cresol, and *m*-aminophenol, one can find that the vibrational frequencies of modes 6a and 1 of *m*-cresol and *m*-aminophenol are redshifted with respect to those of phenol, while the ones of mode 12 are blueshifted. It can be interpreted that the nature and the relative position of the substituent may influence the vibrational frequency of the ring vibration in the S_1 and D_0 states, and the degree of this frequency difference depends on the vibrational pattern.

4. Conclusion

Ab initio and DFT calculations have been applied to predict the optimized molecular structures of the *cis* and *trans* rotamers of *m*-cresol in the S_0, S_1, and D_0 states. The optimized geometries show that *trans* *m*-cresol is more stable than the *cis* rotamer in the S_0 state. Upon the $S_1 \leftarrow S_0$ excitation, the bond lengths of the ring CC bonds are all lengthened, while the ones of the C1–O7 bond are shortened by 0.022 and 0.023 Å for the *cis* and *trans* rotamers. The interaction between the OH group and the ring is much stronger in the D_0 state than that in the S_1 state, and C1–O7 bond exhibits a partial double bond character.

The band origins of *cis* and *trans* *m*-cresol are measured to be $35{,}982 \pm 2$ and $36{,}098 \pm 2\,cm^{-1}$ by the 2C-R2PI method, and their adiabatic IE are determined to be $66{,}933 \pm 5$ and $67{,}084 \pm 5\,cm^{-1}$ by the MATI experiment, respectively. Analysis of the IE of the *o*-, *m*-, *p*-cresol and phenol gives the order as: $p < o < m <$ phenol. Investigation of the spectroscopic features of *cis* and *trans* *m*-cresol in the S_1 and D_0 states shows that different orientations of the OH group from the CH_3 group slightly influence the vibrational frequencies of the in-plane ring deformation.

Acknowledgments

J. Huang acknowledges the financial support from the Doctoral Starting-up Foundation of Central South University (No. 76112156) and the Postdoctoral Science Foundation of Central South University.

References

[1] T. Ichimura, T. Suzuki, J. Photochem. Photobiol. C 1 (2000) 79.
[2] H. Kojima, K. Miyake, K. Sakeda, T. Suzuki, T. Ichimura, N. Tanaka, D. Negishi, M. Takayanagi, I. Hanazaki, J. Mol. Struct. 655 (2003) 185.
[3] A. Oikawa, H. Abe, N. Mikami, M. Ito, J. Phys. Chem. 88 (1984) 5180.
[4] T. Aota, T. Ebata, M. Ito, J. Phys. Chem. 93 (1989) 3519.
[5] R. Tembreull, T.M. Dunn, D.M. Lubman, Spectrochim. Acta A 42 (1986) 899.
[6] A. Oikawa, H. Abe, N. Mikami, M. Ito, Chem. Phys. Lett. 116 (1985) 50.
[7] M. Ito, A. Oikawa, J. Mol. Struct. 126 (1985) 133.
[8] M. Pohl, M. Schmitt, K. Kleinermanns, Chem. Phys. Lett. 177 (1991) 252.
[9] K. Suzuki, S. Ishiuchi, M. Fujii, Faraday Discuss. 115 (2000) 243.
[10] K. Suzuki, Y. Emura, S. Ishiuchi, M. Fujii, J. Electr. Spectrosc. Relat. Phenom. 108 (2000) 13.
[11] J. McMurry, Organic Chemistry, 3rd ed., Brooke/Cole Publishing Company, Belmont, California, 1992.
[12] G. Varsanyi, Assignments of Vibrational Spectra of Seven Hundred Benzene Derivatives, Wiley, New York, 1974.
[13] H. Mizuno, K. Okuyama, T. Ebata, M. Ito, J. Phys. Chem. 91 (1987) 5589.
[14] R. Tembreull, D.M. Lubman, Anal. Chem. 56 (1984) 1962.
[15] R.J. Lipert, S.D. Colson, J. Phys. Chem. 93 (1989) 3894.
[16] E. Fujimaki, A. Fujii, T. Ebata, N. Mikami, J. Chem. Phys. 112 (2000) 137.
[17] M. Mineyama, T. Egawa, J. Mol. Struct. 734 (2005) 61.
[18] T. Isozaki, K. Sakeda, T. Suzuki, T. Ichimura, K. Tsuji, K. Shibuya, Chem. Phys. Lett. 409 (2005) 93.
[19] A. Hirano, H. Tsumanuma, K. Kishi, T. Egawa, J. Mol. Struct. 701 (2004) 9.
[20] P.J. Breen, E.R. Bernstein, H.V. Secor, J.I. Seeman, J. Am. Chem. Soc. 55 (1989) 1958.
[21] M. Ando, S. Yoshiike, T. Suzuki, T. Ichimura, T. Okutsu, M. Ueda, H. Horiuchi, H. Hiratsuka, A. Kawai, K. Shibuya, J. Photochem. Photobiol. A 174 (2005) 194.
[22] K. Müller-Dethlefs, M. Sander, E.W. Schlag, Chem. Phys. Lett. 112 (1984) 291.
[23] L. Zhu, P.M. Johnson, J. Chem. Phys. 94 (1991) 5769.
[24] K.W. Choi, S.K. Kim, D.S. Ahn, S. Lee, J. Phys. Chem. A 108 (2004) 11292.
[25] S.J. Baek, K.W. Choi, Y.S. Choi, S.K. Kim, J. Chem. Phys. 118 (2003) 11040.
[26] J.L. Lin, C. Li, W.B. Tzeng, J. Chem. Phys. 120 (2004) 10513.
[27] M.J. Frisch, et al., GAUSSIAN 03, Revision B. 01, Gaussian, Inc., Pittsburgh, PA, 2003.
[28] M.C. Yoon, Y.S. Choi, S.K. Kim, Chem. Phys. Lett. 300 (1999) 207.
[29] J.L. Lin, W.B. Tzeng, J. Chem. Phys. 115 (2001) 743.
[30] W.A. Chupka, J. Chem. Phys. 98 (1993) 4520.
[31] O. Dopfer, K. Müller-Dethlefs, J. Chem. Phys. 101 (1999) 8508.
[32] X. Song, M. Yang, E.R. Davidson, J.P. Reilly, J. Chem. Phys. 99 (1993) 3224.
[33] H. Ikoma, K. Takazawa, Y. Emura, S. Ikeda, H. Abe, H. Hayashi, M. Fujii, J. Chem. Phys. 105 (1996) 10201.
[34] K. Yosida, K. Suzuki, S. Ishiuchi, M. Sakai, M. Fujii, C.E.H. Dessent, K. Müller-Dethlefs, Phys. Chem. Chem. Phys. 4 (2002) 2534.
[35] B. Zhang, C. Li, H. Su, J.L. Lin, W.B. Tzeng, Chem. Phys. Lett. 390 (2004) 50.
[36] L. Yuan, C. Li, J.L. Lin, S.C. Yang, W.B. Tzeng, Chem. Phys. 323 (2006) 429.
[37] J.L. Lin, K.C. Lin, W.B. Tzeng, J. Phys. Chem. A 106 (2002) 6462.
[38] W.D. Geppert, S. Ullrich, C.E.H. Dessent, K. Müller-Dethlefs, J. Phys. Chem. A 104 (2000) 11864.
[39] C. Li, H. Su, W.B. Tzeng, Chem. Phys. Lett. 410 (2005) 99.
[40] Y. Xie, H. Su, W.B. Tzeng, Chem. Phys. Lett. 394 (2004) 182.